Journal of Experimental Botany, Vol. 61, No. 9, pp. 2383–2393, 2010
doi:10.1093/jxb/erq072 Advance Access publication 8 April, 2010
This paper is available online free of all access charges (see http://jxb.oxfordjournals.org/open_access.html for further details)

Journal of Experimental Botany
www.jxb.oxfordjournals.org

RESEARCH PAPER

Importance of the αC-helix in the cyclic nucleotide binding domain for the stable channel regulation and function of cyclic nucleotide gated ion channels in *Arabidopsis*

Kimberley Chin[1], Wolfgang Moeder[1,2], Huda Abdel-Hamid[1], Dea Shahinas[1], Deepali Gupta[1] and Keiko Yoshioka[1,2,*]

[1] Department of Cell and Systems Biology, University of Toronto, 25 Willcocks Street, Toronto, ON, M5S 3B2 Canada
[2] Center for the Analysis of Genome Evolution and Function (CAGEF), University of Toronto, 25 Willcocks Street, Toronto, ON, M5S 3B2 Canada

* To whom correspondence should be addressed: E-mail: keiko.yoshioka@utoronto.ca

Received 12 October 2009; Revised 3 March 2010; Accepted 4 March 2010

Abstract

The involvement of cyclic nucleotide gated ion channels (CNGCs) in the signal transduction of animal light and odorant perception is well documented. Although plant CNGCs have recently been revealed to mediate multiple stress responses and developmental pathways, studies that aim to elucidate their structural and regulatory properties are still very much in their infancy. The structure–function relationship of plant CNGCs was investigated here by using the chimeric *Arabidopsis AtCNGC11/12* gene that induces multiple defence responses in the *Arabidopsis* mutant *constitutive expresser of PR genes 22* (*cpr22*) for the identification of functionally essential residues. A genetic screen for mutants that suppress *cpr22*-conferred phenotypes identified over 20 novel mutant alleles in *AtCNGC11/12*. One of these mutants, suppressor S58 possesses a single amino acid substitution, arginine 557 to cysteine, in the αC-helix of the cyclic nucleotide-binding domain (CNBD). The suppressor S58 lost all *cpr22* related phenotypes, such as spontaneous cell death formation under ambient temperature conditions. However, these phenotypes were recovered at 16 °C suggesting that the stability of channel function is affected by temperature. *In silico* modelling and site-directed mutagenesis analyses suggest that arginine 557 in the αC-helix of the CNBD is important for channel regulation, but not for basic function. Furthermore, another suppressor mutant, S136 that lacks the entire αC-helix due to a premature stop codon, lost channel function completely. Our data presented here indicate that the αC-helix is functionally important in plant CNGCs.

Key words: Calcium ion channel, CNGC, *cpr22*, cyclic nucleotide gated ion channel, environment, programmed cell death, temperature.

Introduction

For plant survival, cationic nutrients play essential roles in a wide variety of physiological aspects during growth and development. They also play important roles for signal transduction. For example, Ca^{2+} and K^+ fluxes have been reported to be important for abiotic stress as well as biotic stress responses. Uptake and distribution of cationic nutrients mainly relies on membrane-localized cation transporter proteins. Based on genomic sequence data, *Arabidopsis* contains over 150 cation transport proteins (Mäser *et al.*, 2001). Among them cyclic nucleotide-gated ion channels (CNGCs) form a large gene family consisting of 20 members that have been implicated in defence responses, development, and ion homeostasis in plants (Talke *et al.*, 2003; Kaplan *et al.*, 2007; Chin *et al.*, 2009).

CNGCs were first discovered in retinal photoreceptors and olfactory sensory neurons and so far, six CNGC channel genes have been found in mammalian genomes (Zagotta and Siegelbaum, 1996; Zufall *et al.*, 1994).

The structure of CNGCs is similar to that of the voltage-gated outward rectifying K^+-selective ion channel (Shaker) proteins, including a cytoplasmic N-terminus, six membrane spanning regions (S1–S6), a pore domain located between S5 and S6, and a cytoplasmic C-terminus (Zagotta and Siegelbaum, 1996). However, CNGCs are opened by the direct binding of cyclic nucleotides (CN), such as cAMP and cGMP (Fesenko *et al.*, 1985). The CN-binding domain (CNBD) of CNGCs is located at the cytoplasmic C-terminus and exhibits significant sequence similarity to that of protein kinase A, protein kinase G, and the catabolite activator protein of *E. coli* (Bridges *et al.*, 2005). The cytoplasmic C-terminus contains a CNBD that is connected to the pore domain by a C-linker region. Important functional features of CNGCs were extensively studied in animal systems and it has been suggested that the subunit composition of the respective channel complex is an important determinant for functional features such as ligand sensitivity, selectivity, and gating. (Kaupp and Seifert, 2002).

The first plant CNGC, HvCBT1 (*Hordeum vulgare* calmodulin (CaM)-binding transporter), was identified as a CaM-binding protein in barley (Schuurink *et al.*, 1998). Subsequently, several CNGCs were identified from *Arabidopsis* and *Nicotiana tabacum* (Arazi *et al.*, 1999; Köhler *et al.*, 1999). A precise analysis of the CaM binding site has been reported using the tobacco CNGC, NtCBP4 as well as *Arabidopsis* AtCNGC1 and AtCNGC2 and it has been suggested to be located at the αC-helix of the CNBD in these plant CNGCs (Arazi *et al.*, 2000; Köhler and Neuhaus, 2000). However, only a handful of studies on the structure–function analysis of plant CNGCs have so far been published (Hua *et al.*, 2003; Bridges *et al.*, 2005; Kaplan *et al.*, 2007; Baxter *et al.*, 2008).

The *Arabidopsis* mutant *constitutive expresser of PR genes 22* (*cpr*22), which contains a novel chimeric CNGC, AtCNGC11/12, shows environmentally sensitive defence responses, such as heightened salicylic acid (SA) accumulation and a hypersensitive response (HR)-like programmed cell death (Yoshioka *et al.*, 2001; Moeder and Yoshioka, 2009). It has been reported that the expression of *AtCNGC11/12* and its channel activity is attributable for the *cpr22* phenotype (Yoshioka *et al.*, 2006; Baxter *et al.*, 2008). Interestingly, all SA dependent phenotypes, are suppressed under high humidity conditions and enhanced by low humidity (Yoshioka *et al.*, 2001). This type of environmental sensitivity has been reported for various pathogen resistance mutants as well as on defence responses in wild type plants (Moeder and Yoshioka, 2009).

The importance of the interaction between the C-linker domain and the CNBD domain for basic channel function was reported previously by Baxter *et al.* (2008). In addition, it was shown that intragenic mutants of *cpr22* are useful tools to study the structure–function relationship of CNGCs (Baxter *et al.*, 2008). The use of intragenic mutants of *cpr22* were used here for the structure–function study and to reveal the importance of the αC-helix of the CNBD for stable channel function *in planta*.

Materials and methods

Plant growth conditions

Arabidopsis thaliana plants were grown on Pro-Mix soil (Premier Horticulture Inc., Red Hill, PA, USA) in a growth chamber under ambient humidity as described by Silva *et al.* (1999). *Nicotiana benthamiana* plants were grown on the same soil in a greenhouse under a 14:10 h light:dark regimen at 25 °C (day) and 20 °C (night).

Suppressor screening and identification of the S58 mutant

Suppressor no. 58 (S58) was identified in the same screen that was described in Baxter *et al.* (2008).

Trypan blue staining

Leaf samples were taken from 3–4-week-old plants grown on soil. Trypan blue staining was performed as described previously (Yoshioka *et al.*, 2001).

RNA extraction, RT-PCR, and Northern hybridization

Small-scale RNA extraction was carried out using the TRIzol reagent (Invitrogen, Carlsbad, MO, CA), according to the manufacturer's instructions. Reverse transcriptase (RT)-PCR was performed using cDNA generated by SuperScript™ II Reverse Transcriptase (Invitrogen, Carlsbad, MO, CA) according to the manufacturer's instructions. For the detection of CNGC gene expression in *N. benthamiana*, CNGC, and *actin* gene expression in yeast, and *β-tubulin* gene expression in *Arabidopsis*, the same sets of primers described by Baxter *et al.* (2008) were used. For the detection of *PR-1* by RT-PCR, PR-1F: 5′-GCTCTTGTA-GGTGCTCTTGTT-3′ and PR-1R; 5′-CAGCTCTTATTTGTAT-TATTT-3′ were used. Northern hybridization of the *PR-1* gene was performed as previously described (Yoshioka *et al.*, 2006). For the RT-PCR, 25 cycles for each analysis were applied.

Pathogen infection

Infection with *Hyaloperonospora arabidopsidis* isolate Emwa1 was performed as described previously (Yoshioka *et al.*, 2001).

Plasmid construction

The yeast expression vector plasmid pYES2-empty vector (Invitrogen), pYES2-*AtCNGC12*, pYES2-*AtCNGC11/12*, and pYES2-*AtCNGC11/12:E519K* (S73) were constructed as previously described (Yoshioka *et al.*, 2006; Baxter *et al.*, 2008). For pYES2-*AtCNGC11/12:R557C* (S58), total RNA was extracted from S58 and cDNA was generated as described above. cDNA of *AtCNGC11/12:R557C* was then amplified by RT-PCR using primers: BamH-ATG3: 5′-GGGATCCCATGAATCTTCAGAG-GAGAAA-3′ and cDNA14-R1: 5′-CACTATGCTTCAGCCTT-TGC-3′, and then cloned into pGEM-T Easy (Promega, Madison, WI). In the case of pYES2-*AtCNGC11/12:Q543X* (S136), *AtCNGC11/12* cDNA was used as template for PCR using primers: *Bam*H-ATG3: 5′-GGGATCCCATGAATCTTCAGAG-GAGAAA-3′ and Reverse 136 stop mutation R: 5′-TTATCTTT-GAAAGACATTTAA-3′. Both cDNA clones were then subcloned into pYES2 at the *Bam*HI and *Not*I restriction enzyme sites. *AtCNGC:R557C* (S58) cDNA minus stop was generated by RT-PCR using forward 5′-CTCTAGACATGAATCTTCAGAG-GAGAAA-3′ and reverse 5′-AGTCTAGATGCTTCAGCCTTT-GC-3′ primers and subsequently cloned into pGEM-T easy (Promega, Madison, WI). This clone was then subcloned into the *Xba*I site in pMBP3 (Yoshioka *et al.*, 2006; Urquhart *et al.*, 2007). For site-directed mutagenesis, *AtCNGC:R557C* (S58) cDNA was excised using *Xba*I and subsequently subcloned into pBluescript (Stratagene, La Jolla, CA). The point mutation R557I (C1627T)

was introduced into *AtCNGC11/12* cDNA in pBluescript (Baxter *et al.*, 2008) using the QuickChange site-directed mutagenesis kit (Stratagene) according to the manufacturer's instructions. The *AtCNGC11/12:R557I* cDNA was then subcloned into pMBP3 for transient assays in *N. benthamiana*. All constructed plasmids were sequenced for fidelity.

Agrobacterium-*mediated transient expression*

Agrobacterium-mediated transient expression in *N. benthamiana* was performed as described by Urquhart *et al.* (2007). The expression of these genes was confirmed by RT-PCR (see RNA extraction and RT-PCR).

Functional complementation in yeast

K^+ yeast mutant complementation: The K^+-uptake deficient yeast mutant strain CY162 (MAT α, ura3-52, *trk1,2*) was transformed with the empty plasmid pYES2, pYES2-*AtCNGC12*, pYES2-*AtCNGC11/12*, pYES2-*AtCNGC11/12:R557C*, pYES2-*AtCNGC12:R557I* and pYES2-*AtCNGC11/12:Q543X* following the lithium acetate transformation protocol (Ausubel *et al.*, 1987). Yeast transformants were grown in synthetic minimal media supplemented with 0.1 mM KCI (Leng *et al.*, 1999) and hygromycin (5 mg l^{-1}) (Mercier *et al.*, 2004) to suppress background growth. Growth rates were monitored by determining the OD_{600} of the growing yeast cultures at 20 h and 40 h.

Ca^{2+} yeast mutant complementation: A wild-type strain of *S. cerevisiae* W303-1A (Wallis *et al.*, 1989) and the Ca^{2+} channel mutant (*cch1::TRP1* null mutant) strain K927 (Locke *et al.*, 2000) were provided by Dr H Iida (Tokyo Gakugei University). K927 was transformed with pYES2 empty vector, pYES2-*AtCNGC12*, pYES2-*AtCNGC11/12*, pYES2-*AtCNGC11/12:R557C*, pYES2-*AtCNGC12:R557I*, and pYES2-*AtCNGC11/12:Q543X* following the lithium acetate transformation protocol (Ausubel *et al.*, 1987).

To test for complementation of the *cch1* mutation, yeast transformants were grown to logarithmic phase in synthetic minimal media and were diluted to 10^6 cells ml^{-1} and exposed to 20 μM α-mating factor in modified synthetic minimal media containing 100 μM $CaCl_2$ (Muller *et al.*, 2001). 100 μl aliquots of cells were harvested by centrifugation and resuspended in 10 mg ml^{-1} Trypan blue solution at 4, 8, and 12 h. Yeast viability was measured by assessing the ratio of stained to unstained cells under brightfield microscopy. A minimum of 200 cells were counted for each transformant.

Ca^{2+} uptake was measured by the method described by Kurusu *et al.* (2004) with slight modifications. K927 transformants were grown to logarithmic phase in synthetic minimal media and diluted to 10^7 cells ml^{-1}. Cultures were then preincubated for 120 min at 30 °C in 10 mM MES-TRIS buffer (pH 6.0) containing 100 mM glucose. $^{45}CaCl_2$ was added to a final concentration of 72 kBq ml^{-1}. 100 μl aliquots were harvested at 10, 20, and 30 min by centrifugation and washed five times with washing solution (20 mM $MgCl_2$ 0.1 mM $LaCl_3$). Radioactivity in yeast cells were measured using a liquid scintillation counter. All experiments have been conducted with three biological repeats with three technical repeats.

Green fluorescence protein (GFP) visualization by confocal microscopy

Agrobacterium-mediated transient expression in *N. benthamiana* was performed as described in Urquhart *et al.* (2007) at 16 °C and 22 °C. Plants were shifted to 16 °C 12 h after infiltration, and protein stability in either condition was confirmed by GFP expression at 30 h. Small sections of the infiltrated area were excised and used for confocal microscopy. Confocal fluorescence images were acquired using a Leica TCS SP5 confocal system with AOBS® (HCS PL APO CS 40× immersion oil objective; NA, 1.25) with the AOTF for the argon laser (488 nm) set at 35% and the detection window at 500–600 nm (Leica Microsystems Inc., Wetzlar, Germany).

Computational modelling and sequence alignment

The tertiary structure modelling of AtCNGC11/12 was conducted as described previously (Baxter *et al.*, 2008) using the crystallized structure of the cytoplasmic C-terminus of invertebrate CNGC, SpIH (Flynn *et al.*, 2007, PDB no. 2PTM). The protein fold recognition server (Phyre; Kelley and Sternberg, 2009) was used to model the protein coordinates with estimated precision of 100%. All the images were generated using PyMOL (DeLano, 2002).

The sequence alignments of the CNBD amino acid sequences of all 20 *Arabidopsis* CNGCs were aligned using ClustalW (Thompson *et al.*, 1994). The accession numbers of all protein sequences used for the alignment are indicated in the figure legends.

Results

The intragenic suppressor S58 loses cpr22 *related phenotypes under ambient conditions*

The suppressor screen of *cpr22* was reported previously (Baxter *et al.*, 2008). Through this screen more than 20 novel mutant alleles in *AtCNGC11/12* have been discovered so far. One of these mutants, suppressor S58 was found to be morphologically identical to the wild type (wt) plants (Fig. 1a). The homozygosity of the *cpr22* allele in S58 was confirmed by PCR-based marker analysis (data not shown). In contrast to homozygous *cpr22*, S58 is neither lethal, nor shows HR-like spontaneous lesion formation and constitutive *PR-1* gene expression (Fig. 1a, b). Pathogen resistance was evaluated using the oomycete pathogen, *Hyaloperonospora arabidopsidis*, isolate Emwa1, which is virulent for the ecotype Wassilewskija (Ws, the background ecotype of *cpr22*). *cpr22* showed enhanced resistance to Emwa1 (Yoshioka *et al.*, 2006). As predicted, suppressor S58 lost *cpr22*-mediated enhanced resistance to this pathogen (Fig. 1c; see Supplementary Table S1 at *JXB* online). Taken together; it is concluded that suppressor S58 lost all tested *cpr22*-related phenotypes under ambient temperature condition (22 °C). Sequence analysis of the *cpr22* gene (*AtCNGC11/12*) revealed one nucleotide substitution, C to T in the cyclic nucleotide binding domain (CNBD) that caused an amino acid substitution, Arginine 557 to Cysteine (R557C) in S58.

The genetic nature of S58 was evaluated by backcrossing with *cpr22* homozygous plants. As shown in Supplementary Table S2 at *JXB* online, all B_1 (backcross, 1st generation) plants showed *cpr22* heterozygous-like phenotypes, and the following self-pollinated B_2 generation showed a segregation of 1 (wild type like):2 (*cpr22* heterozygous like):1 (lethal). This indicated the semi-dominant nature of this mutation supporting the idea that aforementioned intragenic mutation R557C is the cause of the phenotype suppression. RT-PCR in homozygous *cpr22* and S58 mutants confirmed that there is no significant difference in expression of *AtCNGC11/12* and *AtCNGC11/12:R557C* (data not shown).

The S58 mutation (R557C) does not affect channel function in yeast

Growth enhancement of mutant yeast has been previously demonstrated upon expression of various plant CNGCs (Köhler *et al.*, 1999; Leng *et al.*, 1999; Ali *et al.*, 2006). More recently, it was suggested that AtCNGC11, 12, and AtCNGC11/12 can function as K^+ channels as well as Ca^{2+} channels when expressed in the same systems (Yoshioka *et al.*, 2006; Urquhart *et al.*, 2007). Therefore, it is possible that the loss of *cpr22*-related phenotypes in S58 can be attributed to either a loss in basic ion channel function, or a loss in the constitutive active character of AtCNGC11/12 while still maintaining basic channel function. To address this point, a heterologous expression system using K^+ and Ca^{2+} uptake-deficient yeast mutants was used to evaluate the channel function of AtCNGC11/12:R557C. The *trk1,trk2* K^+ uptake-deficient yeast mutant, CY162 (Leng *et al.*, 1999), transformed with AtCNGC11/12 or AtCNGC11/12:R557C was tested in low external K^+ and in the presence of the cationic antibiotic hygromycin. As shown in Fig. 2a, *AtCNGC11/12* and *AtCNGC12* were able to complement the *trk1,trk2* phenotype compared to the empty vector control. Interestingly, the mutants carrying *AtCNGC11/12:R557C* were also able to complement the *trk1,trk2* phenotype with the same efficiency as *AtCNGC11/12*, whereas another CNBD mutant, S73 (E519K), which affects ion channel function (Baxter *et al.*, 2008) did not, suggesting that the R557C mutation does not affect its basic ion channel function. To explore if this is also the case for Ca^{2+} channel function, a similar complementation analysis was conducted using the Ca^{2+}-uptake yeast mutant strain K927 (*cchl::TRP1*; Locke *et al.*, 2000). *CCH1* has been implicated in Ca^{2+} influx in response to mating pheromones (Fischer *et al.*, 1997). Previously, it has been shown that Ca^{2+} is important for cell death induction by the expression of *AtCNGC11/12* (Urquhart *et al.*, 2007). Therefore, it is possible that only Ca^{2+} channel function is affected by the S58 mutation. However as shown in Fig. 2c by Trypan blue staining, *AtCNGC11/12*, *AtCNGC12*, and *AtCNGC11/12:R557C* rescued this yeast phenotype to comparable levels, indicating that AtCNGC11/12:R557C is functional as a Ca^{2+} ion channel. These data were quantitatively confirmed in Fig. 2b. In addition, $^{45}Ca^{2+}$ uptake analysis was conducted using the same yeast mutant strain. Although the $^{45}Ca^{2+}$ uptake did not reach the same level as wild-type yeast, K927 mutant yeast with *AtCNGC11/12* or *AtCNGC11/12:R557C* had a higher uptake rate of $^{45}Ca^{2+}$ than K927 carrying the empty vector (see Supplementary Fig. S1 at *JXB* online). The same result was observed in four independent experiments. No significant difference between *AtCNGC11/12* and *AtCNGC11/12:R557C* was observed, suggesting that the R557 (S58) mutation does not impair the function of AtCNGC11/12. This result is consistent with the mating pheromone analyses using the same yeast mutant strain (Fig. 2b). Taken together, it was concluded that the mutation *R557C* does not affect basic ion channel function but rather affects the regulation of AtCNGC11/12.

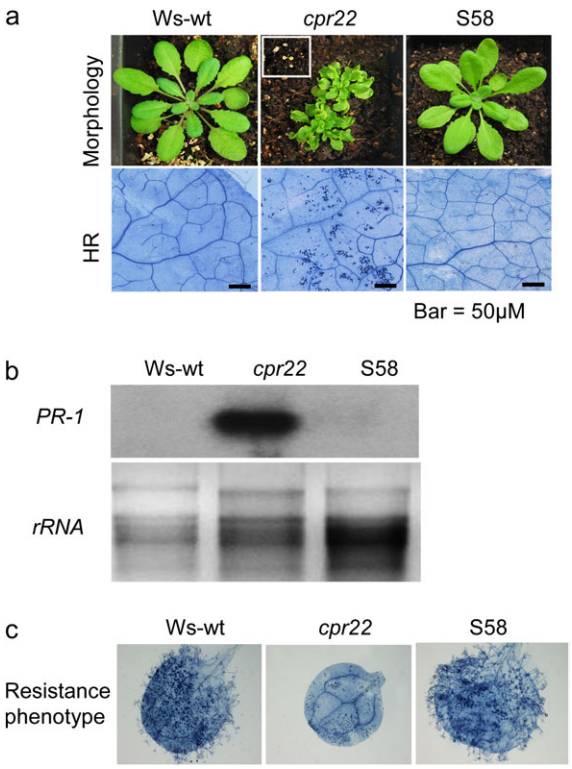

Fig. 1. Characterization of the suppressor mutant S58. (a) Morphological phenotypes and spontaneous HR cell death formation of wilde type (Ws-wt), *cpr22*, and suppressor 58 (S58). A *cpr22* homozygous plant is shown in the white square. Approximately 4-week-old plants were used. (b) Northern blot analysis for *PR-1* gene expression in Ws-wt, *cpr22*, and S58. The samples were taken from approximately 4-week-old plants. Ethidium bromide staining of ribosomal RNA (rRNA; lower panel) served as a loading control. (c) Growth of *Hyaloperonospora arabidopsidis*, isolate Emwa1 in Ws-wt, *cpr22*, and S58. Plants were infected by spraying a conidiospore suspension of 10^6 ml^{-1} on 7-d-old plants. The Trypan blue analysis 8 d after infection was done to visualize pathogen growth.

AtCNGC11/12:R557C *recovers the activity to induce cell death under low temperature*

As mentioned above, *cpr22*-related phenotypes show temperature sensitivity. Relatively high temperatures (>28 °C) can suppress its phenotypes and on the other hand relatively lower temperature (<16 °C) enhanced them (Mosher *et al.*, 2010). Since the *R557C* mutation seems to suppress the constitutive active character of AtCNGC11/12 but not basic ion channel function, the question was asked if lower temperature can restore this constitutive active character (channel activity). Strikingly, a temperature shift from 22 °C to 16 °C induced *cpr22*-like morphology, such as curly leaves 4 d after shift in S58. Chlorosis on leaves, which indicates cell death development, could also be observed (Fig. 3a). Trypan blue staining as well as electrolyte leakage analyses further confirmed cell death development in S58 (Fig. 3a, b). *PR-1* gene expression also recovered after the

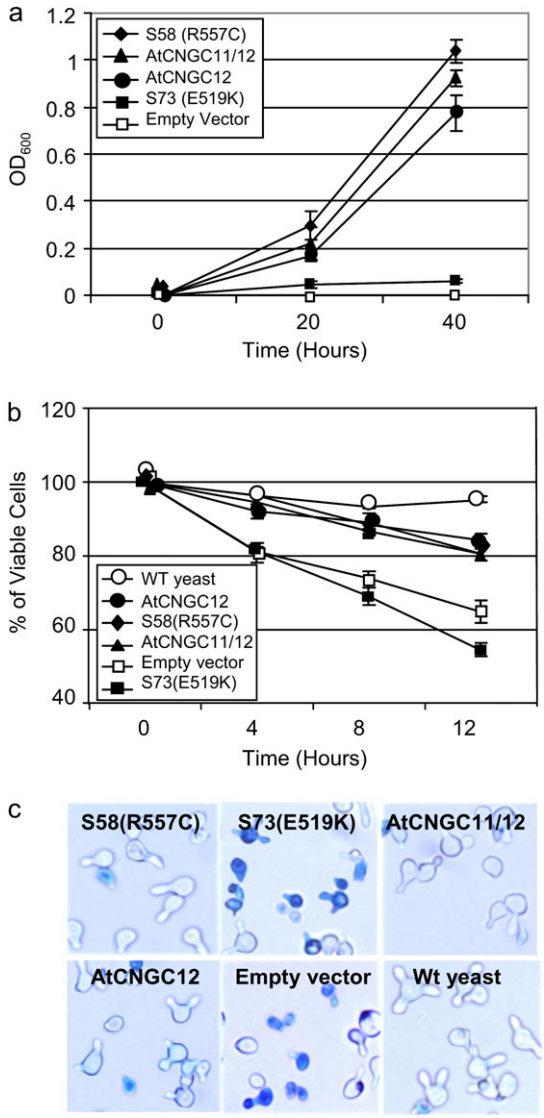

Fig. 2. Yeast complementation analyses. (a) AtCNGC11/12, AtCNGC12, and S58 (AtCNGC11/12:R557C) complemented the K^+-uptake deficient mutant CY162, whereas S73 and the empty vector did not. Data are the average of three biological repeats ±SE. Student's *t* test shows significant differences between the empty vector/S73 and AtCNGC11/12, AtCNGC12, or S58 at 20 h and 40 h (P <0.05). Experiments have been performed more than three times with similar results. (b) AtCNGC11/12, AtCNGC12, and S58 (AtCNGC11/12:R557C) complemented the Ca^{2+}-uptake deficient mutant K927, whereas S73 and empty vector did not. Data are the average of three biological repeats ±SE. Student's *t* test shows significant differences between the empty vector and AtCNGC11/12, AtCNGC12, or S58 at 4, 8, and 12 h (P <0.05).The experiment has been repeated more than three times with comparable results. (c) Yeast viability analysis by Trypan blue staining. AtCNGC11/12, AtCNGC12, and S58 (AtCNGC11/12:R557C) rescued the cell death phenotype of the Ca^{2+}-uptake deficient mutant K927, whereas S73 and empty vector did not.

shift from 22 °C to 16 °C (Fig. 3c), further supporting the temperature sensitivity of this mutant.

To characterize the temperature sensitivity of S58 further (*AtCNGC11/12:R557C*), *Agrobacterium*-mediated transient expression analysis was conducted in *Nicotiana benthamiana*. This is an established system to analyse HR cell death development and has been used to show that *AtCNGC11/12* induces cell death in a synchronized manner (Urquhart *et al.*, 2007). As shown in Fig. 4a, cell death was induced

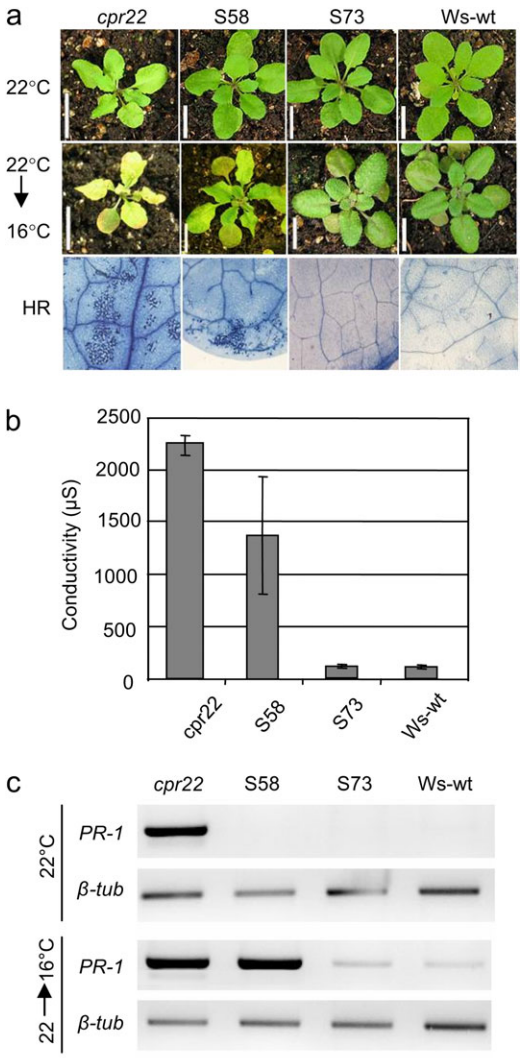

Fig. 3. Temperature sensitivity of *cpr22*-related phenotypes in *cpr22*, S58, S73, and Ws-wt plants after a shift from 22 °C to 16 °C. (a) S58 displayed *cpr22*-morphology after temperature shift. *cpr22* showed enhancement of HR cell death and S58 induced HR cell death and *cpr22*-related phenotypes after the temperature shift. No cell death induction was observed in another intragenic suppressor, S73 and Ws-wt under both conditions. Photographs were taken 7 d after the shift. (b) Quantitative analysis of cell death by electrolyte leakage in *cpr22*, S58, S73, and Ws-wt. Samples were taken 7 d after the shift. (c) RT-PCR analysis of *PR-1* gene expression in *cpr22*, S58, S73, and Ws-wt. Temperature shift induced *PR-1* gene expression in S58, whereas no significant change was observed in S73 and Ws-wt. β-tubulin served as a loading control. Samples were taken 7 d after the shift.

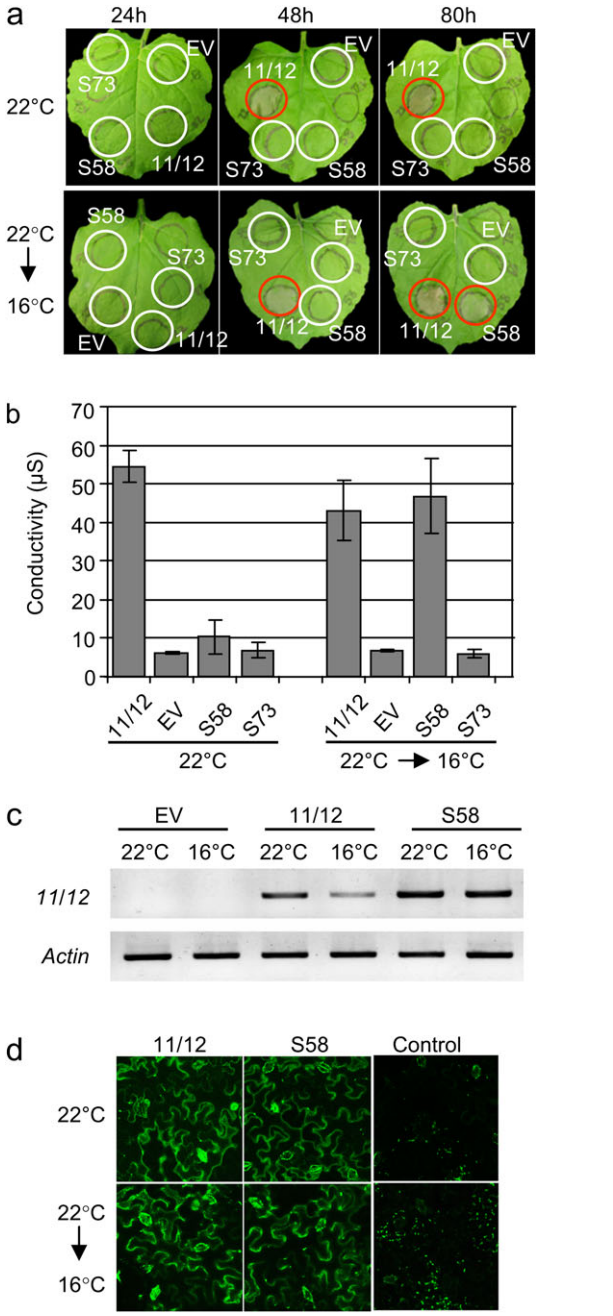

Fig. 4. Temperature sensitivity of cell death induction by transient expression of *AtCNGC11/12*, empty vector, *S58 (AtCNGC11/12:R557C)*, and *S73 (AtCNGC11/12:E519K)* in *Nicotiana benthamiana*. (a) Induction of cell death in *N. benthamiana* 24, 48, and 80 h after *Agrobacterium* infiltration, either shifted from 22 °C to 16 °C at 12 h after *Agrobacterium* infiltration (lower panels) or not shifted (upper panels). Cell death induction was observed in the leaf area expressing *S58*, but not empty vector (EV) or *S73* after the temperature shift. Cell death induced by *AtCNGC11/12* was enhanced by temperature shift. Red circles indicate HR development. (b) Quantitative analysis of cell death in *N. benthamiana* by electrolyte leakage of leaf discs. *S58* expression induced cell death after the temperature shift, but not empty vector (EV) or *S73*. Samples were taken 80 h after *Agrobacterium* infiltration. (c) RT-PCR analysis of leaf discs from *N. benthamiana* leaves expressing *AtCNGC11/12*, *S58* or empty vector (EV). The temperature shift did not significantly affect gene expression of AtCNGC11/12 or AtCNGC11/12*:R557C* in *N. benthamiana* leaf discs. *actin* served as a loading control. Samples were taken 24 h after *Agrobacterium*-infiltration (12 h after the shift). (d) The expression of AtCNGC11/12:GFP and AtCNGC11/12*:R557C*:GFP was not altered by the temperature shift. The samples were taken 30 h after *Agrobacterium* infiltration. The fluorescence of the GFP-fusion proteins was monitored by confocal microscopy.

by the transient expression of *AtCNGC11/12* but not *AtCNGC11/12:R557C* at 22 °C (ambient temperature) indicating the inactivity of AtCNGC11/12:R557C *in planta* under this condition. On the other hand, AtCNGC11/12:R557C recovered cell death induction in plants that were shifted from 22 °C to 16 °C. This was also confirmed quantitatively by electrolyte leakage analysis (Fig. 4b). Transcript and protein levels were not significantly altered by the temperature shift as depicted by RT-PCR (Fig. 4c) and GFP fluorescence (Fig. 4d). Note that while we have observed enhanced cell death in *cpr22* when it was shifted from 22 °C to16 °C (Fig. 3a), there is no significant difference between 22 °C and 16 °C when *AtCNGC11/12* was transiently expressed in *N. benthamiana*. This is probably due to the sampling timing. The samples for Fig. 4b were taken at 80 h after *Agrobacterium* infiltration. At this time point, cell death development induced by transient expression of *AtCNGC11/12* is almost completed and also it is very strong and uniform compared to the mutant itself due to the constitutive CaMV35S promoter.

3D computational modelling of AtCNGC:R557C

In order to predict the role of R557 in channel structure, a computational analysis of the three-dimensional structure of the cytoplasmic C-terminal region was conducted. Previously, the crystal structure of the cytoplasmic C-terminal region of a hyperpolarization-activated cyclic nucleotide-modulated channel, HCN2, has been used as a template (Zagotta *et al.*, 2003, PDB ID: 1Q50, Baxter *et al.*, 2008). The recently published crystal structure of another HCN, SpIH was used here (crystallized with cAMP; Flynn *et al.*, 2007; PDB ID: 2PTM) that possesses higher structural similarity than HCN2 to AtCNGC12 (H Abdel-Hamid and D Shahinas, unpublished data). As shown in Fig. 5a, R557 is located in the middle of the αC-helix in the CNBD. The importance of this αC-helix for cNMP binding has been reported in animal CNGCs (Rehmann *et al.*, 2007). According to the crystal structure of the CNBD of HCN2 in the presence of cAMP, cAMP binds in the anti-configuration between the β-roll and the αC-helix of the CNBD. In our model, the side chain of R557 faces away from the interior of the cNMP binding pocket formed by the β-roll of the CNBD and therefore, likely does not bind to cNMPs directly (Fig. 5a). Hydrophobic interactions between the αC-helix and the base of cNMPs were also postulated to stabilize cNMP binding (Rehmann *et al.*, 2007), further suggesting that the hydrophilic R557 does not directly interact with cNMPs.

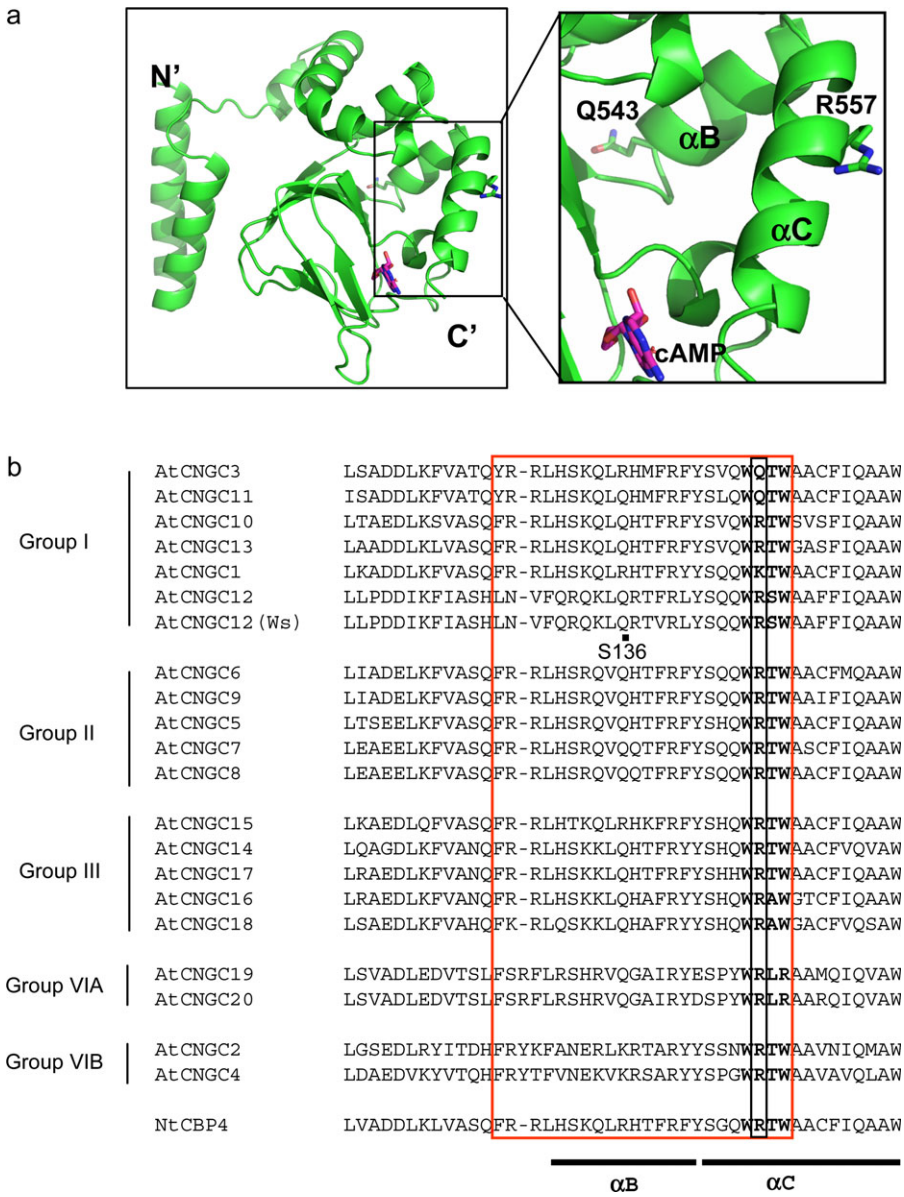

Fig. 5. The location of R557 and Q543 in tertiary structure and amino acid sequence alignment. (a) Ribbon diagram of the cytoplasmic C-terminal region of AtCNGC11/12 (AtCNGC12) (left panel) and close-up of the indicated area of the left panel (right panel). R557 is located in the αC-helix and Q543 is located in the αB-helix of the CNBD. cAMP is indicated by pink colour. (b) Alignment of the area of R557 with 20 *Arabidopsis* CNGCs and tobacco NtCBP4. NCBI:AF079872, AtCNGC3:CAB40128, AtCNGC11:AAD20357, AtCNGC10:AAF73128, AtCNGC13:AAL27505, AtCNGC1:AAK43954, AtCNGC12:AAd23055, AtCNGC12 (Ws ecotype):EU541495, AtCNGC6:AAC63666, AtCNGC9:CAB79774, AtCNGC5:T52573, AtCNGC7:AAG12561, AtCNGC8:NP_173408, AtCNGC15:AAD29827, AtCNGC14:AAD23886, AtCNGC17:CAB81029, ATCNGC16:CAB41138, AtCNGC18:CAC01886, AtCNGC19:BAB02061, AtCNGC20:-BAB02062, AtCNGC2:CAC01740, AtCNGC4:T52574. The black box indicates the position of R557. The red box indicates the CaM binding domain and bold characters highlight the critical four amino acids for the CaM binding suggested by Arazi *et al.* (2000). The location of Q543 (S136) is indicated by a black dot.

A sequence comparison revealed that R557 is conserved in 17 out of 20 *Arabidopsis* CNGCs (Fig. 5b). Only three CNGCs, AtCNGC1, 3, and 11 have a lysine (K) or glutamine (Q) that mediate ionic interactions similarly to arginine (R) in this position. All of them are hydrophilic (hydropathy index: –4.5). Cysteine is slightly polar due to its –SH group but does not mediate any ionic interactions (hydropathy index: +2.5). To address whether a more hydrophobic residue with less polarity than cysteine such as isoleucine (hydropathy index: +4.5) can completely disrupt channel function, AtCNGC11/12:R557I was created by site-directed mutagenesis and it was transiently expressed in *N. benthamiana* to assess cell death induction. As shown in Fig. 6a, cell death is not induced by AtCNGC11/12:R557I at 22 °C, but is recovered at 16 ° C similar to AtCNGC11/12:R557C. The expression of all constructs was confirmed

by RT-PCR (Fig. 6b). Therefore, even by altering R557 to isoleucine complete suppression of channel function at 16 °C could not be obtained.

The αC and αB helices in the CNBD are crucial for channel function

The αC-helix in the CNBD was suggested to play an important role for animal CNGC function/channel gating (Rehmann *et al.*, 2007). However, so far there is almost no report about the importance of the αC-helix in plant CNGCs except one report showing that the CaM binding domain is located in the αC-helix (Arazi *et al.*, 2000). To study the role of the αC-helix in channel function further, another intragenic suppressor mutant, S136, was used that has a premature stop codon at Q543 (C to T point mutation) in the CNBD. Our structural model revealed Q543 to be located at the middle of the αB helix, indicating that S136 does not have the entire αC-helix and only a partial αB helix (Fig. 5a). S136 did not display *cpr22* phenotypes under 22 °C or 16 °C (Fig. 7a). It also lost constitutive expression of *PR-1* and enhanced pathogen resistance (Fig. 7b, c). Furthermore, heterologous expression in the previously mentioned *trk1*,*trk2* K^+ and *cchl* Ca^{2+} yeast mutants revealed that *AtCNGC11/12:Q543X* does not have channel function (Fig. 7d; data not shown). Taken together, these data suggest that the αC- helix and possibly the αB-helix of the CNBD is functionally essential for CNGC function in plants.

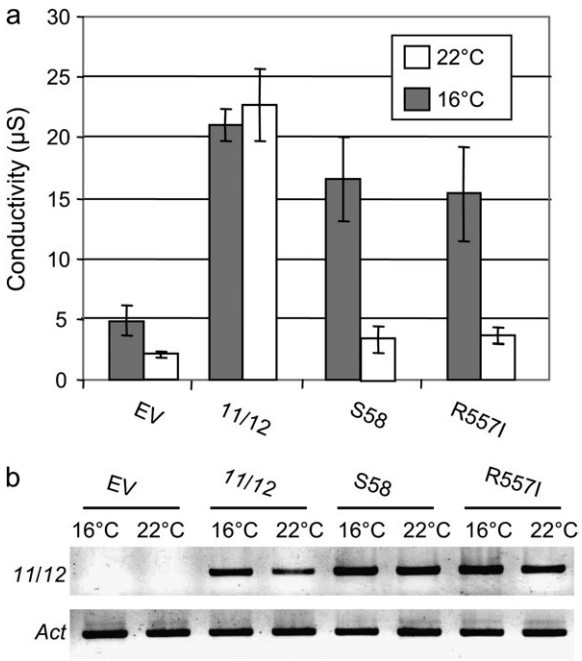

Fig. 6. *AtCNGC11/12:R557I* expression induces cell death similarly to S58 in *Nicotiana benthamiana* at lower temperature. Quantitative analysis of cell death in *N. benthamiana* was assessed by electrolyte leakage of leaf discs. *AtCNGC11/12:R557I* expression induced cell death to the same degree as *AtCNGC11/12:R557C* (S58) after the temperature shift from 22 °C to 16 °C but not at 22 °C. (b) RT-PCR analysis of leaf discs from *N. benthamiana* leaves expressing *AtCNGC11/12*, *S58 (AtCNGC11/12:R557C)*, *AtCNGC11/12:R557I* or empty vector (EV). The temperature shift did not significantly affect gene expression of *AtCNGC11/12*, AtCNGC11/12*:R557C* or AtCNGC11/12*:R557I* in *N. benthamiana* leaf discs. Actin (Act) served as a loading control.

Discussion

Through this study it has been found that R557 in the αC-helix of the CNBD plays an important role in stable channel regulation. Substitution of R557C in the *Arabidopsis* mutant *cpr22* impaired cell death formation and other *cpr22*-related phenotypes suggesting a disruption of channel function. However, the *cpr22*-related phenotypes as well as cell death caused by transient expression of *AtCNGC11/12:R557C* could still be observed under slightly lower temperatures (16 °C) suggesting an alteration in channel regulation rather than channel function. Yeast complementation analysis demonstrated that AtCNGC11/12:R557C maintains its basic channel function for both K^+ and Ca^{2+} conductance, further supporting this notion. R557 is highly conserved in the CNGC family and all residues in this position share similar polarity and hydrophobicity. It has been examined if a change to an even more hydrophobic and less polar residue (R557I) would have a stronger effect that completely disrupts basic channel function. However, this channel remained to be conditional just like AtCNGC11/12:R557C, further strengthening the notion that R557 is important for the regulation of channel activity rather than basic channel function.

In animal systems, it has been reported that cNMPs bind within the pocket formed by the αC-helix and the β-barrel composed of the eight β sheets in the CNBD (Weber and Steitz, 1987; Rehmann *et al.*, 2007). The αC-helix was suggested to function as the lid of this pocket that stabilizes the cNMP binding by forming hydrophobic interactions with the bound cNMP (Rehmann *et al.*, 2007). However, because R557 is hydrophilic, it does not seem to participate directly in cNMP binding. Our computational modelling also supported this notion.

Regarding the role of the αC-helix in plant CNGCs, a 19–20 amino acid sequence of this region was suggested to be the CaM binding domain in AtCNGC1 and AtCNGC2 by Köhler and Neuhaus (2000) using yeast two hybrid analysis. Arazi *et al.* (2000) biochemically demonstrated that a 23 amino acid sequence overlapping with this 19–20 amino acids is the CaM binding domain in the tobacco CNGC, NtCBP4. Furthermore, they reported that the four additional amino acids (W R T/S W) which are located just outside of the 19–20 amino acid sequence are crucial for efficient binding. As shown in the alignment in Fig. 5b, R557 is located in this crucial sequence (indicated by bold characters). Considering the fact that R557C altered its regulation, not the basic channel function itself, it can be hypothesized that R557C displays an alteration in its

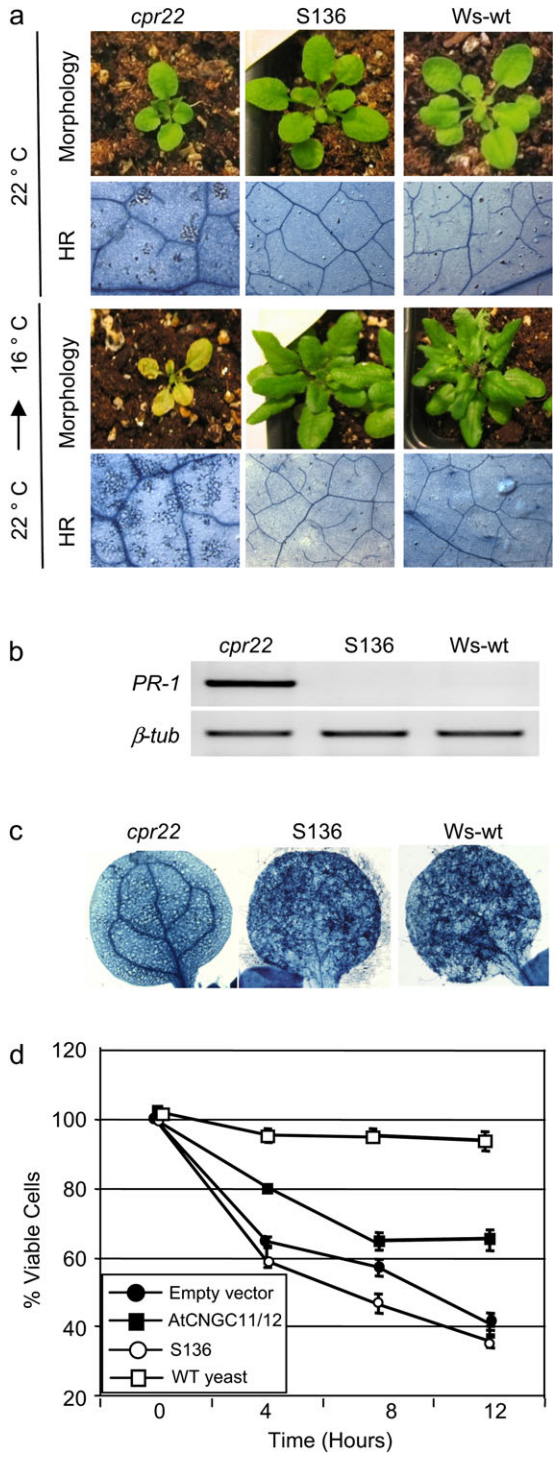

Fig. 7. Characterization of the premature stop codon mutant, S136. (a) Morphological and cell death phenotypes of Ws-wt, *cpr22* and S136 with and without temperature shift. S136, unlike S58 does not induce cell death after a shift from 22 °C to 16 °C. Samples were taken 7 d after the shift. (b) RT-PCR analysis for *PR-1* gene expression in Ws-wt, *cpr22*, and S136. The samples were taken from approximately 4-week-old plants. β-tublin (*β-tub*) served as a loading control. (c) Growth of *Hyaloperonospora arabidopsidis*, isolate Emwa1 in Ws-wt, *cpr22*, and S136. Plants were infected by spraying a conidiospore suspension of 10^6 ml^{-1} on 7-d-old plants. The Trypan blue analysis 8 d after infection was done to visualize pathogen growth. (d) Yeast complementation analysis using the Ca^{2+}-uptake deficient mutant K927. Only *AtCNGC11/12* but not S136 (*AtCNGC11/12: Q543X*) rescued the K927 phenotype. Data are the average of three biological repeats ±SE. Student's *t* test shows a significant difference between AtCNGC11/12 and both empty vector and S136 at 12 h (P <0.05).The experiment has been repeated more than three times with similar results.

binding affinity to CaM which causes an alteration to the regulation of its function. Considering the importance of CaM in regulating this channel group, our finding is significant. Biochemical studies that aim to identify the CaM interactions with AtCNGC11/12 (AtCNGC12) are underway.

The experimental results involving of suppressor S136 was unexpected, since the deletion of the part of the CNBD that includes the CaM binding site has been reported to enhance the AtCNGC1 channel function in yeast (Ali *et al.*, 2006). Ali *et al.* (2006) demonstrated that two deletion constructs of AtCNGC1 showed enhanced K^+ channel function in a yeast complementation analysis. They hypothesized that the binding of the negative regulator CaM does not occur in these deletion constructs thereby promoting channel activity. Based on our computational modelling, the deletion of S136 is positioned between these two constructs (data not shown). However, we did not see any channel function using both K^+ and Ca^{2+} yeast mutants in the case of S136, suggesting the importance of the αC-helix and possibly the αB-helix for its basic channel function. This discrepancy could be due either to differences in regulatory properties of different AtCNGC subunits or to unknown structural changes caused by the different deletion positions used in both studies. As of now, the answer remains unknown and further analyses will be required to understand these differences.

In this study, it has been demonstrated that R557 in the αC-helix of the CNBD of CNGCs plays an important role for channel regulation and that the αC-helix and possibly αB-helix are crucial for plant CNGC channel function. It has been proposed that the αC-helix binds to both cNMP and CaM as a mechanism to regulate CNGC channel gating (Arazi *et al.*, 2000). Our data here demonstrates the importance of the αC-helix in a plant CNGC for the first time. Further precise structural and biochemical studies to elucidate the role of the αC-helix are underway.

Supplementary data

Supplementary data are available at *JXB* online.

Supplementary Fig. S1. Ca^{2+}-uptake analysis using Calcium-45 AtCNGC11/12 and S58 (AtCNGC11/12:R557C) partially complemented the Ca^{2+}- uptake deficient mutant K927, whereas the empty vector did not.

Acknowledgements

This project was supported by a Discovery Grant from NSERC (Natural Science and Engineering Research Council of Canada), CFI (Canadian Foundation for Innovation), and ORF (Ontario Research Fund) to KY, and a graduate student fellowship from Egyptian government to HA.
We thank Dr Leon Kochian at Cornell University for providing the CY162 yeast mutant strain. We also thank Dr Hidetoshi Iida at Tokyo Gakugei University and Dr Kyle W Cunningham at Johns Hopkins University for providing the K927 yeast mutant strain as well as for technical advice. For their patient technical assistance, we thank Dr Ali Rashid at the University of Connecticut, Dr Kazuyuki Kuchitsu, and Dr Takamitsu Kurusu at the Tokyo University of Science. We also would like to thank Mr William Urquhart for his assistance for plasmid construction.

References

Ali R, Zielinski RE, Berkowitz GA. 2006. Expression of plant cyclic nucleotide-gated cation channels in yeast. *Journal of Experimental Botany* **57,** 125–138.

Arazi T, Sunkar R, Kaplan B, Fromm H. 1999. A tobacco plasma membrane calmodulin-binding transporter confers Ni^{2+} tolerance and Pb^{2+} hypersensitivity in transgenic plants. *The Plant Journal* **20,** 171–182.

Arazi T, Kaplan B, Fromm H. 2000. A high-affinity calmodulin-binding site in tobacco plasma-membrane channel protein coincides with a characteristic element of cyclic nucleotide-binding domains. *Plant Molecular Biology* **42,** 591–601.

Ausubel FM, Bent R, Kingston RE, Moore DD, Seidman JG, Smith JA, Struhl K. 1987. *Current protocols in molecular biology*. New York: John Wiley and Sons.

Baxter J, Moeder W, Urquhart W, Shahinas D, Chin K, Christendat D, Kang HG, Angelova M, Kato N, Yoshioka K. 2008. Identification of a functionally essential amino acid for Arabidopsis cyclic nucleotide gated ion channels using the chimeric *AtCNGC11/12* gene. *The Plant Journal* **56,** 457–469.

Bridges D, Fraser ME, Moorhead GBG. 2005. Cyclic nucleotide bindning proteins in the *Arabidopsis thaliana* and *Oryza sativa* genomes. *BMC Bioinformatics* **11,** 6.

Chin K, Moeder W, Yoshioka K. 2009. Biological roles of cyclic-nucleotide-gated ion channels in plants: what we know and don't know about this 20 member ion channel family. *Botany* **87,** 668–677.

DeLano WL. 2002. *The PyMOL molecular graphics system*. Palo Alto, CA, USA: DeLano Scientific.

Fesenko EE, Kolesnikov SS, Lyubarsky AL. 1985. Induction by cyclic GMP of cationic conductance in plasma membrane of retinal rod outer segment. *Nature* **313,** 310–313.

Fischer M, Schnell N, Chattaway J, Davies P, Dixon G, Sanders D. 1997. The *Saccharomyces cerevisiae CCH1* gene is involved in calcium influx and mating. *FEBS Letters* **419,** 259–262.

Flynn GE, Black KD, Islas LD, Sankaran B, Zagotta WN. 2007. Structure and rearrangements in the carboxy-terminal region of SpIH channels. *Structure* **15,** 671–682.

Hua BG, Mercier RW, Zielinski RE, Berkowitz GA. 2003. Functional interaction of calmodulin with a plant cyclic nucleotide gated cation channel. *Plant Physiology and Biochemistry* **41,** 945–954.

Kaplan B, Sherman T, Fromm H. 2007. Cyclic nucleotide-gated channels in plants. *FEBS Letters* **581,** 2237–2246.

Kaupp UB, Seifert R. 2002. Cyclic nucleotide-gated ion channels. *Physiological Reviews* **82,** 769–824.

Kelley LA, Sternberg MJE. 2009. Protein structure prediction on the web: a case study using the Phyre server. *Nature Protocols* **4,** 363–371.

Köhler C, Merkle T, Neuhaus G. 1999. Characterization of a novel gene family of putative cyclic nucleotide- and calmodulin-regulated ion channels in *Arabidopsis thaliana*. *The Plant Journal* **18,** 97–104.

Köhler C, Neuhaus G. 2000. Characterisation of calmodulin binding to cyclic nucleotide-gated ion channels from *Arabidopsis thaliana*. *FEBS Letters* **4710,** 133–136.

Kurusu T, Sakurai Y, Miyao A, Hirochika H, Kuchitsu K. 2004. Identification of a putative voltage-gated Ca^{2+} permeable channel (OsTPC1) involved in Ca^{2+} influx and regulation of growth and development in rice. *Plant and Cell Physiology* **45,** 693–702.

Leng Q, Mercier RW, Yao W, Berkowitz GA. 1999. Cloning and first functional characterization of a plant cyclic nucleotide-gated cation channel. *Plant Physiology* **121,** 753–761.

Locke EG, Bonilla M, Liang L, Takita Y, Cunningham KW. 2000. A homolog of voltage-gated Ca^{2+} channels stimulated by depletion of secretory Ca^{2+} in yeast. *Molecular Cell Biology* **29,** 6686–6694.

Mäser P, Thomine S, Schroeder JI, *et al*. 2001. Phylogenetic relationships within cation transporter families of *Arabidopsis*. *Plant Physiology* **126,** 1646–1667.

Mercier RW, Rabinowitz NM, Gaxiola RA, Ali R, Berkowitz GA. 2004. Use of hygromycin hypersensitivity of a K^+ uptake yeast mutant as a functional assay of plant cyclic nucleotide gated cation channels. *Plant Physiology and Biochemistry* **42,** 529–536.

Moeder W, Yoshioka K. 2009. Environmental sensitivity in pathogen resistant Arabidopsis mutants. In: Yoshioka K, Shinozaki K, eds. *Signal crosstalk in plant stress responses*. Ames, IA: Wiley-Blackwell, 113–135.

Mosher S, Moeder W, Nishimura N, Jikumaru Y, Joo SH, Urquhart W, Klessig DF, Kim SK, Nambara E, Yoshioka K. 2010. The lesion mimic mutant *cpr22* shows alterations in abscisic acid signaling and abscisic acid insensitivity in a salicylic acid-dependent manner. *Plant Physiology* **152,** 1–13.

Muller EM, Locke EG, Cunningham KW. 2001. Differential regulation of two Ca^{2+} influx systems by pheromone signaling in *Saccharomyces cerevisiae*. *Genetics* **159,** 1527–1538.

Rehmann H, Wittinghofer A, Bos JL. 2007. Capturing cyclic nucleotides in action: snapshots from crystallographic studies. *Nature Reviews Molecular Cell Biology* **8,** 63–73.

Schuurink RC, Shartzer SF, Fath A, Jones RL. 1998. Characterization of a calmodulin-binding transporter from the plasma membrane of barley aleurone. *Proceedings of the National Academy of Sciences, USA* **95,** 1944–1949.

Silva H, Yoshioka K, Dooner HK, Klessig DF. 1999. Characterization of a new *Arabidopsis* mutant exhibiting enhanced disease resistance. *Molecular Plant–Microbe Interactions* **12,** 1053–1063.

Talke IN, Blaudez D, Maathuis FJM, Sanders D. 2003. CNGCs: prime targets of plant cyclic nucleotide signaling? *Trends in Plant Science* **8,** 286–293.

Thompson JD, Higgins DG, Gibson TJ. 1994. CLUSTAL W: improving the sensitivity of progressive multiple sequence alignment through sequence weighting, position specific gap penalties and weight matrix choice. *Nucleic Acids Research* **22,** 4673–4680.

Urquhart W, Gunawardena AHLAN, Moeder W, Ali R, Berkowitz GA, Yoshioka K. 2007. The chimeric cyclic nucleotide-gated ion channel ATCNGC11/12 constitutively induces programmed cell death in a Ca^{2+} dependent manner. *Plant Molecular Biology* **65,** 747–761.

Wallis JW, Chrebet G, Brodsky G, Rolfe M, Rothstein R. 1989. A hyper-recombination mutation in *S. cerevisiae* identifies a novel eukaryotic topoisomerase. *Cell* **58,** 409–419.

Weber IT, Steitz TA. 1987. Structure of a complex of catabolite gene activator protein and cyclic AMP refined at 2.5 Å resolution. *Journal of Molecular Biology* **198,** 311–326.

Yoshioka K, Kachroo P, Tsui F, Sharma SB, Shah J, Klessig DF. 2001. Environmentally-sensitive, SA-dependent defence response in the *cpr22* mutant of *Arabidopsis*. *The Plant Journal* **26,** 447–459.

Yoshioka K, Moeder W, Kang HG, Kachroo P, Masmoudi K, Berkowitz G, Klessig DF. 2006. The chimeric Arabidopsis CYCLIC NUCLEOTIDE-GATED ION CHANNEL11/12 activates multiple pathogen resistance responses. *The Plant Cell* **18,** 747–763.

Zagotta WN, Siegelbaum SA. 1996. Structure and function of cyclic nucleotide-gated channels. *Annual Review of Neuroscience* **19,** 235–263.

Zagotta WN, Olivier NB, Black KD, Young EC, Olson R, Gouaux E. 2003. Structural basis for modulation and agonist specificity of HCN pacemaker channels. *Nature* **425,** 200–205.

Zufall F, Firestein S, Shepherd GM. 1994. Cyclic nucleotide-gated ion channels and sensory transduction in olfactory receptor neurons. *Annual Review of Biophysics and Biomolecure Structure* **23,** 577–607.